

# New Methods for Modeling and Analysis of Digital Images

E.P. Akishina, P.G. Akishin, V.V. Ivanov, B.F. Kostenko

*Laboratory of Information Technologies,  
Joint Institute for Nuclear Research, 141980, Dubna, RUSSIA*

## Abstract

New methods for simulation and analysis of digital images are developed at Laboratory of Information Technologies. This work considers their applications to the solving of specific problems in the area of medicine and nuclear power engineering.

For the last years much attention has been paid to research aimed at the creation of a device for obtaining a picture of the microstructure of the skin's surface layer without a dangerous influence on the patient. A new approach to application of optical coherent tomography (OCT) has been recently developed at the Institute of Applied Physics of RAS (Nizhniy Novgorod) for a real-time analysis of the skin's microstructure, and a corresponding device has been designed [1].

Fig. 1 shows a scheme of the device for obtaining OCT-images designed on the basis of Michaelson interferometer [1]. The analyzed sample is placed in one of the arms of

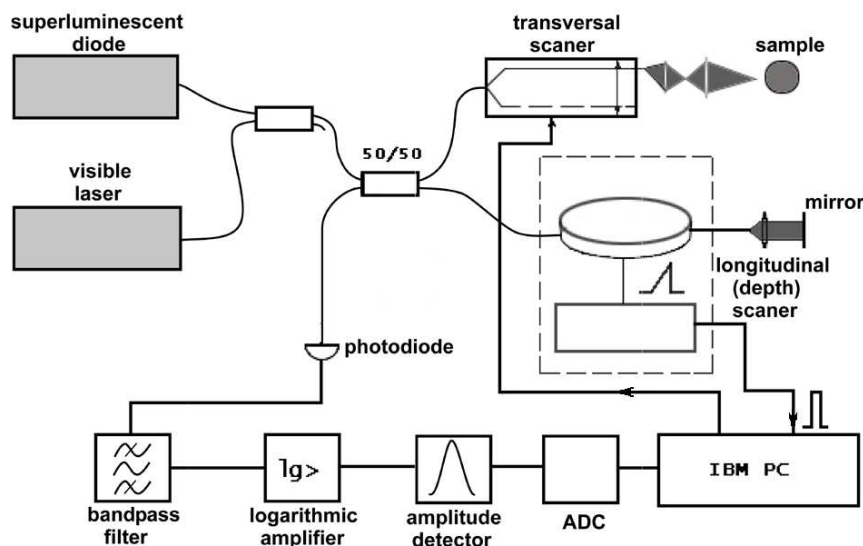


Figure 1: Schematic view of the fast-scanning OCT-device

the interferometer as a scattering object. The interferential signal is proportional to a refraction coefficient of a non-scattering component inside the analyzed sample. With the help of an interface card the OCT-device is connected to PC whose specialized software allows one to control the measuring procedure. Visualization of the signal allows one to receive a real-time optical tomograms, including several images all at once from the same spot of patient's skin.

The analysis of OCT-images has shown that their distortions are caused mainly by light dispersion in the surface skin layer. In order to make diagnosis more reliable, one should improve the quality of digital images by means of their filtering with no loss of useful information. No needed result has been obtained by applying filters from the wide-known commercial package IDL [2]. That is why an original algorithm has been developed for filtering images with sharp jumps of intensity [3]. A description of the filter can be found below.

Let  $\zeta(x)$  be intensity of a non-distorted signal in point  $x = (x_1, x_2)$ . We get a noised signal  $\xi$  resulting from stochastic scattering of light by the skin tissue. The stochastic scattering effect can be described by a random noise  $\eta$ , that should be filtered from the measured signal  $\xi$ . The filter gives the estimate  $\tilde{\zeta}(x)$  of the initial signal  $\zeta(x)$  obtained on the basis of the measured data  $\{\xi^\mu(x), \mu = 1, \dots, M\}$ , where  $M$  is a number of OCT images measured from the same place on patient's skin.

We assume that noise  $\eta(x)$  satisfies the following conditions: 1)  $\eta$  is additive in every point of the digital image, 2)  $\eta$  has a similar distribution over the whole image, 3)  $\eta$  has a zero average value, 4)  $\eta$  has  $\sigma^2$  dispersion, 5) there is no correlation between two different points of the image.

From conditions 1) and 2) we get:

$$\xi^\mu(x) = \zeta(x) + \eta^\mu(x), \quad \mu = 1, \dots, M.$$

To filter the image, let us represent it on a discrete lattice and consider the intensities of the signal in its nodes. Let us select a working window with a center in the analyzed point  $c = (c_1, c_2)$ . The nodes within the window can be written as  $\{x | x^\nu = z^\nu + c, \nu = 1, \dots, N\}$ . Index  $\nu = 1, \dots, N$  denotes a number of the point, and  $z^\nu = (z_1^\nu, z_2^\nu)$  its coordinates with respect to center  $c$ .

Estimation  $\tilde{\zeta}(c)$  received on the basis of measured signals  $\{\xi^\mu(x), \mu = 1, \dots, M\}$ , is determined by a linear filter:

$$\tilde{\zeta}(c) = \sum_{\mu=1}^M \sum_{\nu=1}^N W^\mu(z^\nu) \xi^\mu(z^\nu + c), \quad (1)$$

where  $W^\mu(z^\nu)$  are weights, for computations of which special cases are considered, namely, when on the input of the filter only not defected signals come or else stochastic noise only.

We approximate the initial signal within the selected window on the finite set of basic functions of two variables with respect to center  $c$ :

$$\bar{\zeta}(x) = \sum_{k=1}^K A_k g_k(x - c) = \sum_{k=1}^K A_k g_k(z). \quad (2)$$

In case of a polynomial basis we have

$$\bar{\zeta}(x_1, x_2) = \sum_{0 \leq n+m \leq L} A_{nm} (x_1 - c_1)^n (x_2 - c_2)^m. \quad (3)$$

If the signal is not noised off and is a polynomial of power not bigger  $L$ , we demand the estimation  $\tilde{\zeta}$  should coincide with the initial signal, i.e.  $\zeta = \tilde{\zeta}$ . Thus, for signals  $\zeta(x)$

which are linear combinations of basic functions  $g_k(x - c)$  we have:

$$g_k(0) = \sum_{\mu=1}^M \sum_{\nu=1}^N W^\mu(z^\nu) g_k(z^\nu), \quad k = \overline{1, K}, \quad (4)$$

or

$$g_k(0) = \left( \sum_{\mu=1}^M \mathbf{W}^\mu \right) \cdot \mathbf{g}_k, \quad k = \overline{1, K}, \quad (5)$$

where

$$\mathbf{W}^\mu = (W^\mu(z^1), \dots, W^\mu(z^N)), \quad \mathbf{g}_k = (g_k(z^1), \dots, g_k(z^N)). \quad (6)$$

Besides, we demand that in absence of the main signal  $\zeta$  the filter should minimize the dispersion caused by noise  $\eta$ :

$$D_M = E \left[ \sum_{\mu=1}^M \sum_{\nu=1}^N W^\mu(z^\nu) \eta^\mu(z^\nu + c) \right]^2 = \sum_{\mu=1}^M \|\mathbf{W}^\mu\|^2 \sigma^2. \quad (7)$$

In order to find weights  $W^\mu(z^\nu)$ , when fulfilling condition (5), we minimize the quadratic form:

$$\sum_{\mu=1}^M \|\mathbf{W}^\mu\|^2 = \mathbf{W}_0 \cdot \mathbf{W}_0 = \|\mathbf{W}_0\|^2, \quad \mathbf{W}_0 = (\mathbf{W}^1, \dots, \mathbf{W}^M).$$

Taking into account Cauchy-Bunyakovsky inequality, we have:

$$\frac{\|\sum_{\mu=1}^M \mathbf{W}^\mu\|^2}{M} \leq \sum_{\mu=1}^M \|\mathbf{W}^\mu\|^2. \quad (8)$$

Equality in (8) can take place only if

$$\mathbf{W}^\mu = \frac{\sum_{\mu'=1}^M \mathbf{W}^{\mu'}}{M}. \quad (9)$$

Let us present vector  $\sum_{\mu'=1}^M \mathbf{W}^{\mu'}$  as follows:

$$\sum_{\mu'=1}^M \mathbf{W}^{\mu'} = \mathbf{U} + \sum_{k=1}^K \beta_k \mathbf{g}_k,$$

where  $\mathbf{U}$  is orthogonal to all the vectors of the set  $\{\mathbf{g}_k\}$ . Then condition (5) can be rewritten as follows:

$$\sum_{k'=1}^K \beta_{k'} (\mathbf{g}_{k'} \cdot \mathbf{g}_k) = g_k(0), \quad k = 1, \dots, K. \quad (10)$$

Taking into account interrelationship (8) for functional  $\|\mathbf{W}_0\|^2$ , we have:

$$\|\mathbf{W}_0\|^2 \geq \frac{\|\mathbf{U}\|^2 + \|\sum_{i=1}^K \beta_i \mathbf{g}_i\|^2}{M}. \quad (11)$$

This means that minimum of  $\|\mathbf{W}_0\|^2$  is reached if  $\mathbf{U} = 0$ . In this case:

$$\mathbf{W}^\mu = \frac{\sum_{i=1}^K \beta_i \mathbf{g}_i}{M} \quad \text{for } \mu = 1, \dots, M. \quad (12)$$

Thus, all vectors  $\{\mathbf{W}^\mu\}$  are identical.

As a result, the equality (5) assumes the following form:

$$g_k(0) = M \mathbf{W}_M \cdot \mathbf{g}_k, \quad k = 1, \dots, K. \quad (13)$$

The desired weights of filter (1) are determined from the system (13).

The considered algorithm is intended for filtering smooth images. In this case, as coefficients  $\beta_i$  in (10) do not depend upon the center of the working window, the weights  $W^\mu(z_\nu) = W(z_\nu)$  are determined only once.

If the image has sharp intensity jumps, a histogram of intensity is built on the basis of points in the working window for all measured data  $\{\xi^\mu(x), \mu = 1, \dots, M\}$ . The histogram can have at least two clusters. Summing in (1) is done only on points that belong to cluster  $\Omega$  containing a central point of the window. Equality (5) takes the form:

$$g_k(0) = M \sum_{z^\nu \in \Omega} W(z^\nu) g_k(z^\nu), \quad k = \overline{1, K}. \quad (14)$$

The set of corresponding weights  $W$  is calculated by system (10) for each particular case. A similar procedure is used to filter the points located near the image boundaries.

Table 1: Comparison of various filtering algorithms

Algorithms	Lie	Median	Smoothing	SF
$d_1$	52.9	102.0	51.1	8.1
$d_2$	23.2	16.6	15.6	3.8

Table 1 gives the results of comparison of the developed stochastic filter (SF) in case of using one image with known filtering algorithms taken from the IDL package [2]. As a measure for comparison of various algorithms, values  $d_1$  and  $d_2$  were used:  $d_1 = \max_{i=1}^N |\zeta_i - \tilde{\zeta}_i|$ ,  $d_2 = \sqrt{\sum_{i=1}^N |\zeta_i - \tilde{\zeta}_i|^2 / N}$ , where  $N$  is a total quantity of points in the image, and  $\zeta_i = \zeta(c_i)$  and  $\tilde{\zeta}_i = \tilde{\zeta}(c_i)$  are a real signal and its estimate in point  $c_i$ , correspondingly. Clearly, the new filter noticeably exceeds the IDL filters.

In addition, as the OCT-device optical system allows one to get several images simultaneously from the same place of the patient's skin, this provides a way for improving the filtering quality in  $\sqrt{M}$  [4] times. For qualitative and quantitative estimates of filtration results, both model data and real OCT-images were used.

Fig. 2 shows a result of applying a group filtration algorithm to real OCT-images. Simultaneously five OCT-images were used. One of the images is given on Fig. 2 (left plot): it contains  $250 \times 250$  points. To filter, a round window of the radius  $R_w = 4$  and approximating polynomials of power  $L = 2$  were used. Fig. 2 (right plot) shows a result of

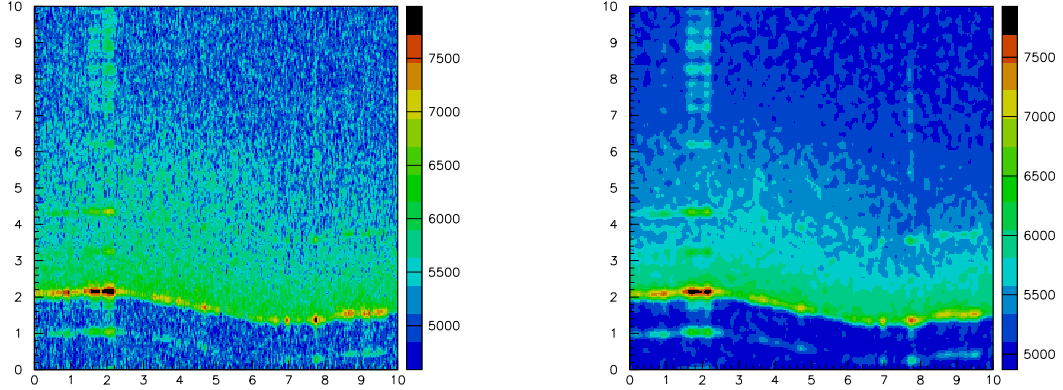


Figure 2: Initial OCT-image ( $250 \times 250$  points) and filtered image on the basis of 5 images obtained from the same spot of the skin:  $R_w = 4$  and  $L = 2$

applying a group filter. It is seen that the filtration has allowed one to specify clearly all the characteristic features of the skin spot under study and noticeably suppress random noise.

Another direction of the research in simulation and analysis of digital images concerns the development of new methods to study the process of forming the surface structures in uranium dioxide resulting from its strong burn-up in nuclear power plants. This process attracts widespread attention in view of the possibility of its catastrophic influence on the safe conditions of the operation of modern atomic power plants. The process is of particular interest for researchers because the mechanism of forming such structures and behavior of corresponding parameters have been poorly understood.

The analyzed structures are formed due to radioactive fission of nuclei - one of the processes of decaying heavy radionuclides. When decaying, several neutrons and considerable energy ( $\sim 210$  MeV) are released. The energy is released mainly as a kinetic one ( $\sim 170$  MeV) of two nuclear fragments which fly away in opposite directions with a high speed. When they pass a crystal lattice of a solid, the fragments form defects, the so-called tracks. On the microphotographs of the surface the tracks are given as pores (dark spots).

Presently, there is no realistic physical model for description of the process under consideration, no adequate mathematical apparatus has been developed for its study. A new approach has been developed at LIT on the basis of cellular automata (CA) for simulation and analysis of microphotographs of surface structures formed at strong uranium fuel burn-up. The cellular automata as a mathematical tool became quite effective for research in complex collective processes in biology and physics.

In our case, microphotographs (with 1250 times enlargement) for burn-up degrees of 16.2, 42.6, 54.8 and 65.0 GWd/tM (Gigawatt-day per (metric) ton metal) were used as a source material. It corresponds the time of fuel stay in a reactor during 323, 953, 1266 and 1642 days, respectively. As an example, Fig. 3 gives a microphotograph of an as-polished sample for a burn-up degree of 16.2 GWd/tM. Initial images were converted into black-

and-white ones by tuning brightness and contrast (see Fig. 4). Then the black-and-white images were converted into ASCII-files: black and white points (cells) were designate by 0 and 1, correspondingly. Those files are the CA chessboard.

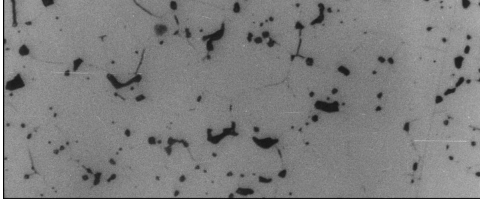


Figure 3: Scanned microphotograph of the surface of an as-polished sample for 16.2 GWd/tM burn-up degree 16.2 GWd/tM



Figure 4: Black-and-white representation of the microphotograph of the surface of an as-polished sample for 16.2 GWd/tM burn-up degree 16.2 GWd/tM

On the CA basis, algorithms have been developed which were used for extraction from the microphotographs of quantitative characteristics of the surface structures corresponding to various degrees of the  $\text{UO}_2$  burn-up as well as for simulation of the spatial time dynamics of those structures in the process of the  $\text{UO}_2$  burn-up [8]-[12]. The CA algorithms of image processing are used to determine the quantitative characteristics of pores (the number of cells in a pore, the coordinates of its center, average and maximal pore radius), to select pores with a predetermined number of cells and to calculate their boundary length, to study a statistic independence of some parts of the microphotographs. The CA algorithms of modeling the surface structure dynamics were applied to modeling the processes of restoration (anti-etching) and etching as well as for description of the pore formation process (on the basis of Ising model).

Here we present the results received with CA algorithms for calculation of the number of cells in pores and for modeling the chemical etching process.

Figs. 5 and 6 show distributions of the numbers of cells in pores (black spots) on the surface of a fixed size, corresponding to burn-up degrees of 16.2 and 42.6, and Figs. 7 and 8 give corresponding black-and-white images. Figs. 9 and 10 show distributions of the numbers of cells in pores for burn-up degrees of 54. and 65.0 GWd/tM, and Figs. 11 and 12 give corresponding black-and-white images.

The distributions under consideration show a characteristic evolution of the fuel's surface layer depending upon a burn-up degree, namely:

1) with growing the burn-up degree from 16.2 up to 65.0 GWd/tM one can observe a systematic growth of pore numbers;

2) with growing the burn-up degree from 16.2 to 54.8 GWd/tM there is a destruction of large-sized pores (their "decay" into smaller pores), as well as formation of small-sized pores takes place;

3) at transition from burn-up degree 54.8 to 65.0 GWd/tM one observes an aggregation of small spots into spots of a larger size; in this case in the distribution one observes a characteristic peak corresponding to the most probable spot size ( $\sim 40$ -50 pixels); it should be noted that the distribution shown on Fig. 10 is approximated quite well by a log-normal law.

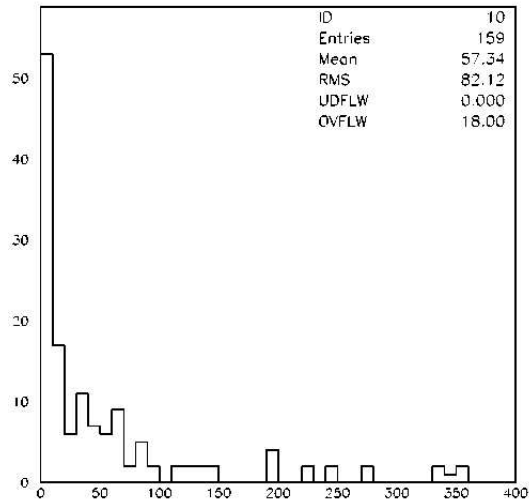


Figure 5: Distribution of the number of cells in pores for burn-up degree 16.2 GWd/tM

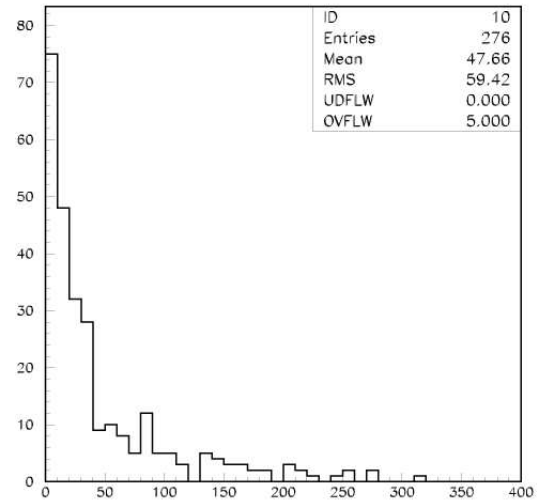


Figure 6: Distribution of the number of cells in pores for burn-up degree 42.6 GWd/tM

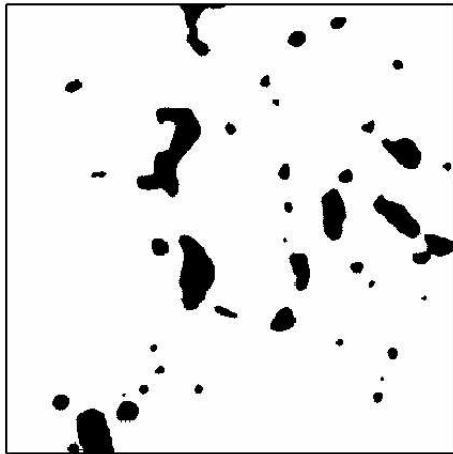


Figure 7: Black-and-white representation of the microphotograph at burn-up degree 16.2 GWd/tM

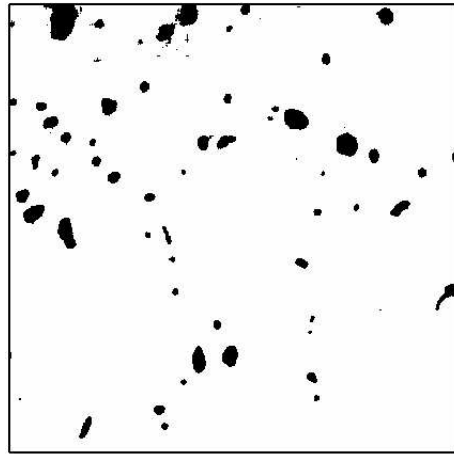


Figure 8: Black-and-white representation of the microphotograph at burn-up degree 42.6 GWd/tM

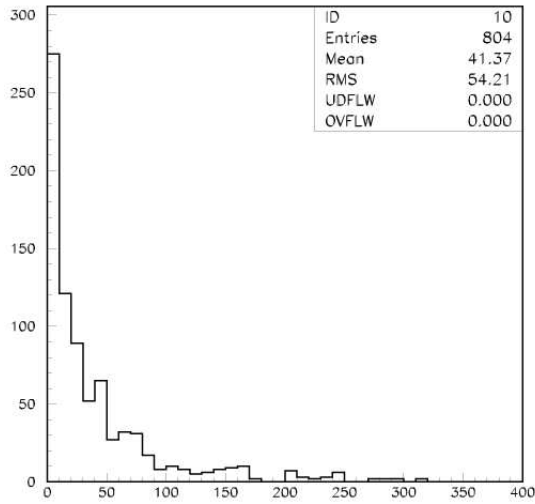


Figure 9: Distribution of the number of cells in pores for burn-up degree 54.8 GWd/tM

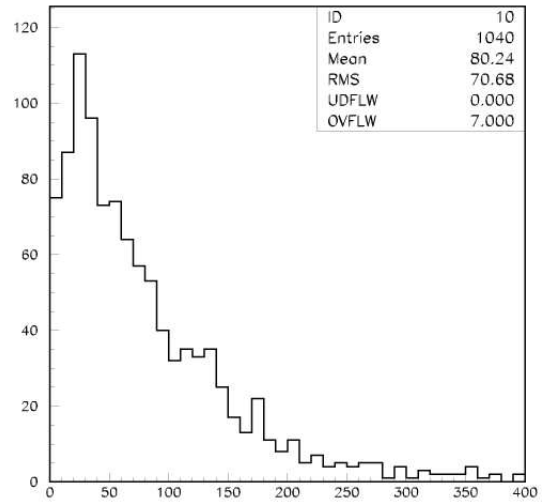


Figure 10: Distribution of the number of cells in pores for burn-up degree 65 GWd/tM

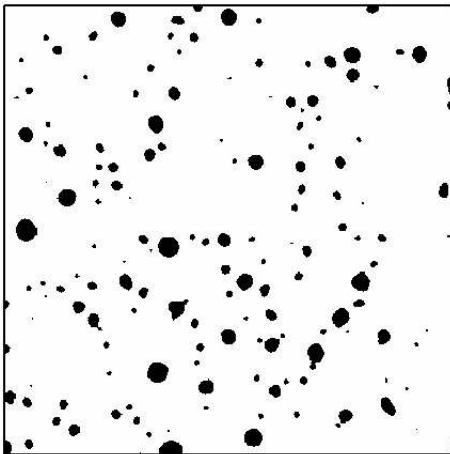


Figure 11: Black-and-white representation of the microphotograph at 54.8 GWd/tM degree burn-up

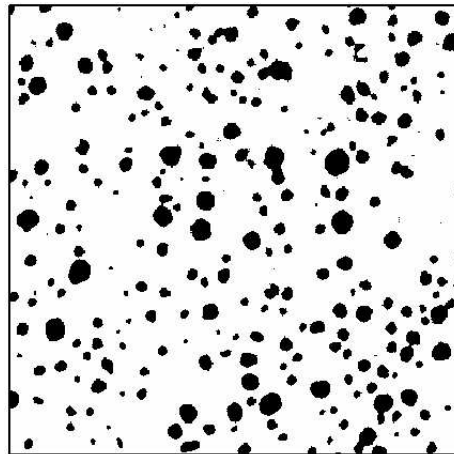


Figure 12: Black-and-white representation of the microphotograph at 65 GWd/tM degree burn-up

The distribution corresponding to the burn-up degree 65.0 GWd/tM shows that small pores begin joining together thus forming pores of bigger size. This fact proves that the system tends to equilibrium. Clearly, this result is of particular importance for understanding the subsequent dynamics of the whole system and particularly the evolution of the surface structure.

The observation of latent tracks is possible only with the help of transmission electron microscope. In early days tracks were investigated exactly this way. For visual research on tracks by means of the optical microscope the procedure of increasing the track size and their visualization have been developed. The most popular and widely used chemical etching is based on the fact that the points of damage (latent tracks) are subjects to dissolving by a chemically aggressive reagent. A sample is placed in a chemical reagent that dissolves the defects thus increasing the track size.

It should be noted that the procedure of the chemical etching is not understood to a nicety yet. To date, there is no model that could render well enough this process. We have proposed an algorithm based on CA that allows simulation of the  $\text{UO}_2$  etching (see details in [12]).

Fig. 13 shows an initial sample which was used for simulation of the etching process. Besides pores, it contains artificially applied points corresponding to primary defects formed nearby the cracks. Such type defects are responsible for the process of chemical etching.

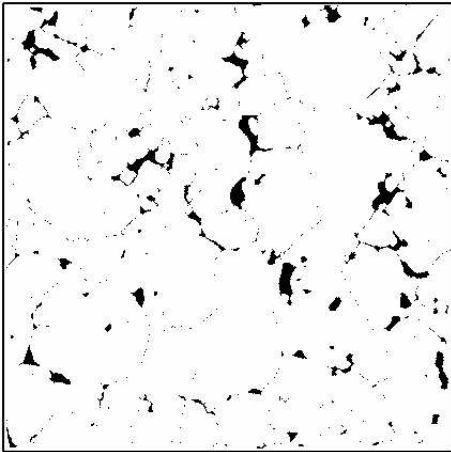


Figure 13: Initial sample that was used for modeling the etching process

The initial image is subject to processing by the CA algorithm in series several times. Figs. 14 and 15 show the results of applying this CA for 10 and 20 iterations of the algorithm, respectively. The result given on Fig. 15 demonstrates quite well the peculiar features of the microphotograph corresponding to a real chemical etching.

The formation of the structures due to strong  $\text{UO}_2$  burn-up known also as a RIM-effect is a result of numerous physical processes (see [5]–[7] and references therein). That is why the corresponding dynamics should be of essentially nonlinear and casual character what can lead to formation of fractal structures. In order to get additional information about the effect, we applied the fractal analysis methods to research of the images of RIM-effect region that correspond to different  $\text{UO}_2$  burn-up degrees  $\text{UO}_2$  [10].

Let  $\delta$  be a characteristic length of the basis element. By calculating the number of  $N(\delta)$  elements (a square or a circle) required for covering the boundaries of the analyzed

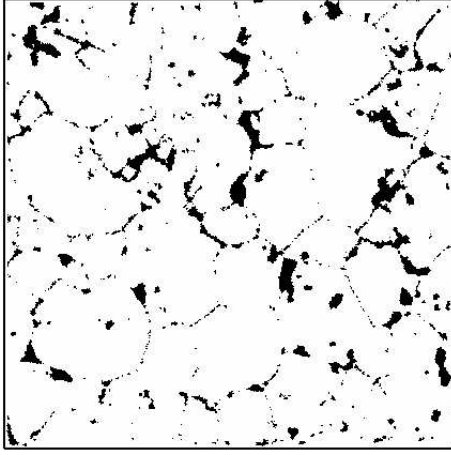


Figure 14: Result of modeling the process of etching with CA after 10 iterations

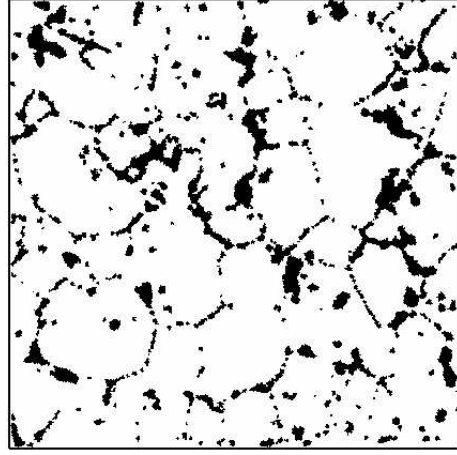


Figure 15: Result of modeling the process of etching with CA after 20 iterations

image, we get its approximate length  $L(\delta) = N(\delta) \cdot \delta$ . The analysis has shown that  $L(\delta)$  is described quite well by dependence  $L(\delta) = a \cdot \delta^{1-D}$ . Thus, we get an equality:

$$N(\delta) \cdot \delta = a \cdot \delta^{1-D}, \quad (15)$$

where  $a = L_0$  is a constant corresponding to  $\delta = 1$ . From (15) we get a relationship:

$$\ln N(\delta) = \ln a - D \ln \delta. \quad (16)$$

Changing the characteristic length  $\delta$  from its minimal value up to some maximal value, we determine in Eq. (16) a tilt  $D$  that is a desired fractal dimensionality.

Table 2 gives results of the fractal analysis for the microphotographs of as-etched samples.

Table 2: Results of the fractal analysis for the microphotographs of as-etched samples

Fractal dimension	Average degree of burn-up 16.2 GWd/tM	Average degree of burn-up 43.9 GWd/tM	Average degree of burn-up 54.8 GWd/tM	Average degree of burn-up 65 GWd/tM
$D_1$ ((module boundaries)	1.34	<b>1.14</b>	<b>1.06</b>	<b>1.17</b>
$D_2$ (150-200 $\mu$ from module boundaries)	1.40	1.24	1.24	<b>1.08</b>
$\langle D \rangle$ (average value 0-200 $\mu$ from module boundaries)	1.37	<b>1.18</b>	<b>1.15</b>	<b>1.13</b>

One can see that the fractal dimension lessens with growing the burn-up degree. It should be noted that the transition from a not damaged (not-rim) to re-formed (rim) structure can be considered, respectively, as a transition from a non-organized microstructure to a self-organized one. The latter appears at high burn-up degree, when a drastic

increase of values  $D_1$ ,  $D_2$  and  $\langle D \rangle$  takes place (in Table 2, samples with fractal dimension  $\leq 1.18$  correspond to the RIM-transition). The obtained result coincides with the results of optical and electronic microscopy of fuel of nuclear reactors conforming that the RIM-structure formation begins at burn-up degrees  $\geq 40 \text{ GWd/tM}$ .

Thus, one can see that the fractal dimension is an important quantitative characteristics for the description of the RIM-process formation. The obtained result also serves as a conformation of a nonlinearity and a stochastic character of the process under study.

## References

- [1] Gelikonov V.M., Gelikonov G.V., Gladkova N.D., Kuranov R.V., Nikulin N.K., Petrova G.A., Pochinko V.V., Pravdenko K.I., Sergeev A.M., Feldchtein F.I., Khanin Ya.I., Shabanov D.V., "Письма в ЖЭТФ", том 61, номер 1-2, 1995, p. 149-153.
- [2] IDL, version 5.0, Reference guide, vol. 1/2, March, 1997 Edition.
- [3] P.G.Akishin, E.P.Akishina, P.Akritas, I.Antoniou, J.Ioannovich and V.V.Ivanov: *Filtering Digital Images of Human Skin Micro-Structure*, "Computer Physics Communications", vol. **126**, No. **1/2**, 2000, p.1-11.
- [4] P.G.Akishin, E.P.Akishina, P.Akritas, I.Antoniou, J.Ioannovich, V.V.Ivanov: *Multi-Sample Stochastic Filtering of Digital Images of Skin Micro-Structure*, "Computational Methods in Sciences & Engineering", vol. **2**, no. **1-2**, 2002, pp.117-124.
- [5] Hj. Matzke, J. Spino: *Formation of the rim structure in high burn-up fuel*, Jour. of Nucl. Materials, 1997, vol. 248, pp. 170-179.
- [6] M. Kinoshita, T. Sonoda, S. Kitajima, A. Sasahara, E. Kolstad, Hj. Matzke, V.V. Rondinella, A.D. Stalios, C.T. Walker, I.L.F. Ray, M. Steindlin, D. Halton, C. Ronchi: *High burn-up rim project. Irradiation and examination to investigate rim-structured fuel*, Proc. Int. Conf. on LWR Fuel Performance, Amer. Nucl. Soc., Park City, April 9-14, 2000, pp. 590-603.
- [7] Chan Bock Lee, Youn Ho Jung: *An attempt to explain the high burn-up structure formation mechanism in UO<sub>2</sub> fuel*, Jour. of Nucl. Materials, 2000, vol. 279, pp. 207-215.
- [8] I.Antonoiu, E.P.Akishina, V.V.Ivanov, B.F.Kostenko, A.D.Stalios: *Cellular Automata Modeling of High Burn-up Structures*, "Computational Methods in Applied Sciences and Engineering", (in press).
- [9] I.Antonoiu, E.P.Akishina, V.V.Ivanov, B.F.Kostenko, A.D.Stalios: *Cellular Automata Study of High Burn-up Structures*, "Chaos, Solitons & Fractals" 18 (2003) 1111-1128.
- [10] I.Antonoiu, E.P.Akishina, V.V.Ivanov, B.F.Kostenko: *Cellular Automata Modelling and Fractal Analysis of High Burn-up Structures in UO<sub>2</sub>*, "WSEAS Transactions on Computers", Issue 4, Vol. 2, October 2003, pp. 1061-1066.
- [11] E.P.Akishina, V.V.Ivanov, B.F.Kostenko: *Cellular Automata Approach to Investigation of High Burn-up Structures in Nuclear Reactor Fuel*, "Particles and Nuclei, Letters", (2005), Vol. 2, No. 1(124)pp. 59-72.
- [12] Е.П. Акишина, В.В. Иванов, Б.Ф. Костенко: *Изучение структур сильного выгорания двуокиси урана с помощью клеточных автоматов: алгоритмы и программы*, Сообщения ОИЯИ, P11-2003, Dubna, 2003, стр. 1-39.